Available online at www.sciencedirect.com
SCIENCE DIRECT®
Applied Energy 79 (2004) 201–214
APPLIED ENERGY
www.elsevier.com/locate/apenergy

Modeling hourly diffuse solar-radiation in the city of São Paulo using a neural-network technique

Jacyra Soares [a,*], Amauri P. Oliveira [a], Marija Zlata Božnar [b], Primož Mlakar [b], João F. Escobedo [c], Antonio J. Machado [a]

[a] *Group of Micrometeorology, Department of Atmospheric Sciences, University of São Paulo, Cidade Universitaria, Rua do Matão 1226, São Paulo, SP 05508-900, Brazil*
[b] *Joef Stefan Institute and AMES d.o.o., Jamova 39, Ljubljana SI-1000, Slovenia*
[c] *Laboratory of Solar radiation, Department of Environmental Sciences, UNESP, Botucatu, Brazil*

Accepted 22 November 2003
Available online 13 February 2004

Abstract

In this work, a perceptron neural-network technique is applied to estimate hourly values of the diffuse solar-radiation at the surface in São Paulo City, Brazil, using as input the global solar-radiation and other meteorological parameters measured from 1998 to 2001. The neural-network verification was performed using the hourly measurements of diffuse solar-radiation obtained during the year 2002. The neural network was developed based on both feature determination and pattern selection techniques. It was found that the inclusion of the atmospheric long-wave radiation as input improves the neural-network performance. On the other hand traditional meteorological parameters, like air temperature and atmospheric pressure, are not as important as long-wave radiation which acts as a surrogate for cloud-cover information on the regional scale. An objective evaluation has shown that the diffuse solar-radiation is better reproduced by neural network synthetic series than by a correlation model.

Keywords: Hourly diffuse solar radiation; Perceptron neural network; São Paulo City

* Corresponding author. Tel.: +55-11-3091-4711; fax: +55-11-3091-4714.
E-mail address: jacyra@usp.br (J. Soares).

0306-2619/$ - see front matter © 2004 Elsevier Ltd. All rights reserved.
doi:10.1016/j.apenergy.2003.11.004

Nomenclature

Abbreviations

MBE	mean bias error
MLP	multilayer perceptron neural-network
RMSE	root mean-square error

Symbols

E_{DF}	diffuse energy component at the Earth's surface, per unit of area and per hour
E_G	total flux of energy received from the Sun at the Earth's surface, per unit of area and per hour
E_T	flux of solar radiation received at the top of atmosphere, per unit of area per hour
$K_{DF} = E_{DF}/E_G$	diffuse fraction
$K_T = E_G/E_T$	clearness index
LW	hourly flux of long-wave atmospheric emission
RH	hourly relative-humidity
SAA	hourly solar azimuth-angle
SEA	hourly solar elevation-angle
SZA	hourly solar zenith-angle
t_S	*t*-statistic proposed by Stone
t_c	critical value of *t*-statistic relative to a level of confidence of 95%
VP	hourly partial-pressure of the water in the atmosphere

1. Introduction

The importance of knowing the temporal and spatial variations of diffuse solar-radiation has been explored in several papers [1–3]. However, solar-radiation data are frequently available from only a few stations and over short periods of time. An alternative procedure to obtain solar-radiation data is using numerical modeling, but the main problem is the need for an appropriate representation of cloud effects [4]. As pointed out by Oliveira et al. [3], these problems are particularly severe in tropical regions, like Brazil, where cloud activity is a dominant feature of local climate and the solarimetric network is sparse with most of the stations located in urban areas.

A common alternative is to estimate the diffuse component of solar radiation from empirical relationships derived from statistical analyses of direct and global solar-radiation temporal series observed [5–9]. These empirical models are based on the correlation between hourly, daily and monthly values of the clearness index (energy flux received from the Sun over the energy flux received at the top of the atmosphere) and diffuse fraction (diffuse/total solar radiation). The empirical relationships used to estimate the hourly diffuse component of solar radiation are, in general, expressed in terms of *n*th-degree polynomials which are dependent on lati-

tude, precipitable water-content, atmospheric turbidity, surface albedo, altitude and solar elevation angle [10,11].

Oliveira et al. [3] used measurements of global and diffuse solar radiations in the City of São Paulo (Brazil) to derive empirical models to estimate hourly, daily and monthly diffuse solar radiation from values of the global solar radiation, based on the correlation between the diffuse fraction and clearness index (K_T). The correlation models performed well for daily and monthly values. However, in the case of the hourly values, the expressions derived for São Paulo performed poorly. According to Erbs et al. [7], the empirical models obtained from hourly value correlations do not produce good results because the hourly values of global solar-radiation are very sensitive to cloud type. In the case of São Paulo, cloud information (sky fraction, type and altitude) with hourly resolution is not available.

Here, to avoid this short-cut inherent in correlation models, the hourly diffuse solar-radiation was assumed to be a non-linear function of other relatively easily measured meteorological parameters and estimated using a multilayer perceptron (MLP) neural-network with nonlinear transfer function [12,13]. The meteorological data, used in this work, were observed between 1998 and 2002 at the City of São Paulo (Brazil).

The neural-network technique has been previously applied to several studies of radiation with hourly resolution, as for example, to estimate hourly global solar-radiation [14] and global photosynthetically-active radiation [15]: however, to the knowledge of the authors, the neural-network technique has never been applied to estimate hourly values of diffuse solar-radiation.

The performance of the MLP neural-network was objectively tested using mean bias error (MBE), root mean-square error (RMSE) and *t*-statistic (t_S) [16].

2. Meteorological data set

Several surface meteorological parameters have been regularly measured in São Paulo City, Brazil, since May 1994. The measurements were taken on a platform located at the top of the ''Instituto de Astronomia, Geofísica e Ciências Atmosféricas da Universidade de São Paulo'' at the University Campus, in São Paulo western side, at 744 m amsl (23°33′35″S, 46°43′55″W), with a sampling frequency of 0.2 Hz (12 min^{-1}) and stored at 5-min intervals. All data were checked, questionable data were removed and the shadow-band blocking-effects on the diffuse solar-radiation values were taken into consideration [17]. All solar radiation quantities used in this work are expressed in units of megajoules per unit of area (MJ m^{-2}) and correspond to the flux of energy per hour.

The measured parameters were: (1) global solar-radiation, (2) diffuse solar-radiation, (3) long-wave atmospheric emission, (4) air temperature, (5) relative humidity and (6) atmospheric pressure.

Global solar irradiance and its diffuse component were measured by a pyranometer model 8-48 and model 2, respectively, both built by Eppley Lab. Inc. These

sensors were calibrated periodically [17] using as secondary standard another spectral precision pyranometer model 2 – (Eppley).

The diffuse component of the solar radiation was measured using a shadow-band device developed by the Laboratory Solar Radiation of UNESP, named "movable detector device" [18]. Compared with other devices commercially available, this new device has a low cost and is much easier to operate and performs well for low latitude locations.

The long-wave atmospheric emission was measured by a Precision Infrared Radiometer (Model PIR Pyrgeometer) from Eppley, which is an instrument used for performing hemispherical, broadband, infrared radiative-flux measurements, using a thermopile temperature-difference. Its composite transmission window is about 4–50 μm. The model PIR pyrgeometer comes with a battery-powered resistance network that provides a voltage that expresses the radiative-flux contribution of the temperature reservoir.

The long-wave data used here was obtained considering only the manufacturer's optional battery-compensated output. Some studies, however, have shown the need for additional corrections for the Eppley model PIR pyrgeometer data [19–21] besides the manufacture's adjustment. These corrections are based on measurements of case and dome temperatures. Unfortunately, restrictions in the channel number of the data-logger unit precluded dome-temperature measurements and consequently the measurements used here cannot be corrected as suggested by Dana [19], Fariall et al. [20] and Reda et al. [21].

Fairall et al. [20] have shown that the exclusive use of the manufacturer's instruction can lead to errors in the total flux up to 5% of the total ($\sim$20 Wm^{-2}), making the measurements used here accurate to that extent. This error could be a serious problem when long-wave data are used, for instance, to perform energy balances or to get surface temperatures. However, this error is not expected to compromise qualitatively the neural-network application performed here because the long-wave radiation is responsible only for a small part of the diffuse solar-radiation behaviour.

The air temperature and relative humidity were estimated using a pair of thermistors from Vaisalla. A pressure transducer from Setra measured the atmospheric pressure.

Some results obtained here will be compared to the results obtained by Oliveira et al. [3]. The solar-radiation data set used by Oliveira et al. [3] was taken on the same platform as the data used in this work and during the period of 62 months, from May 1, 1994 to June 30, 1999.

3. Neural network

There are several types of artificial neural networks, and the selection of the proper one is a crucial point for the investigated problem. Here, the three-layer perceptron artificial neural-network with non-linear transfer function, which has been shown to be an effective alternative to more traditional statistical techniques, is

used [22]. Hornik [23] has shown that the MLP can be trained to approximate virtually any smooth (including highly nonlinear) measurable function. Unlike other statistical techniques, the MLP makes no prior assumptions concerning the data distribution.

According to Rumelhart et al. [12], the multilayer perceptron consists of a system of simple interconnected neurons, or nodes: it is a model representing a nonlinear mapping between an input vector and an output vector. The nodes are connected by weights and output signals, which are a function of the sum inputs to the node modified by a simple non-linear transfer or activation function. It is a superposition of many simple non-linear transfer functions that enables the MLP to approximate extremely non-linear functions [24].

The topology of the three-layer perceptron neural-network used here consists of several neurons in the input layers (each one representing one input feature), several neurons in the hidden layer and one neuron in the output layer representing the modeled parameter. Neurons have a non-linear sigmoid transfer-function $f(x) = 1/(1 + e^{-x})$. The standard back-propagation algorithm [12] was used for training the MLP.

In short, the method of construction of the MLP-based model consists of [25]: (i) feature and pattern selection, (ii) determination of proper MLP topology, (iii) training and (iv) verification.

The purpose of feature determination and pattern-selection techniques is to condense the most relevant information from the database making the training process more efficient and the results significantly better.

In all the experiments performed here, the *training set* (learning and optimization dataset) consists of the period from 1998 to 2001. The *testing set*, taken from the year 2002, was employed for testing the validity of the generated series and also for comparison with the correlation method [3].

The optimization data set consisted of a randomly-selected 10% of patterns from the original training set and was used during the training process to periodically test the MLP performance using the "unknown" data set to determine the MLP's generalization capabilities. The final network was the one that gave the smallest error on the optimization data set and not on the training set.

4. Experiments

Here, three different experiments were performed and all the networks were trained with patterns from almost 4 years long (January 1998 → September 2001) and verified using 1-year long dataset (year 2002). Each measured or calculated parameter of this database represents a potential MLP input-feature. The diffuse solar-radiation (E_{DF}) or its fraction over global solar-radiation (K_{DF}) is the MLP output-feature. Every hourly interval vector of all selected parameters represents a pattern [26].

First, the database was analyzed using feature-determination techniques [27] to decide which parameters are the most relevant for the MLP construction. Two

techniques were used – contribution factors and saliency metric – both based on the analysis of weight of MLP trained with all the available and random parameters and all available patterns.

The contribution factor of a particular parameter is the sum of the absolute weights guiding from the correspondent input neuron to the neurons in the hidden layer. The highest scores indicate the most relevant parameters to be input features for the final network.

The saliency metric, on the other hand, is based on the weights of the whole neural network, not only the input layers [27].

First, the analysis was performed using all available parameters: the six measured parameters plus the year, local time, true day, true hour, local time sunset, local time sunrise, true time sunset, true time sunrise, day duration, solar zenith angle, solar elevation angle, solar hour angle, solar azimuth angle, correction factor of diffuse solar radiation [18], partial pressure of the water vapour in the atmosphere, mixing ratio, theoretical solar radiation at the atmosphere top, fraction of diffuse over global solar-radiations and a random parameter. After that, the process was repeated using the nine best ones: diffuse solar radiation (E_{DF}), theoretical solar-radiation at the atmosphere top (E_T), global solar-radiation (E_D), long-wave atmospheric emission (LW), relative humidity (RH), partial pressure of the water vapour in the atmosphere (VP), theoretical solar elevation angle (SEA), theoretical solar zenith angle (SZA) and theoretical solar azimuth angle (SAA), from 1998 to 2002 plus random parameter.

Figs. 1 and 2 show the results obtained using, respectively, the contribution factor and saliency metric for the most important parameters to be used as the neural-network input. It is interesting to note that the long-wave radiation is as important a parameter as the global solar-radiation in both methods. Physically the long-wave radiation short-scale variations, associated with the presence of clouds and theirs effects over the solar diffuse radiation, were captured by the neural network. Therefore, the long-wave radiation measured at the surface seems to be a good surrogate for the cloud cover information over the region. On the other hand, tra-

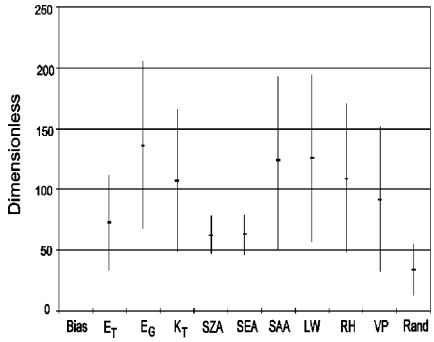

Fig. 1. Final contribution factors.

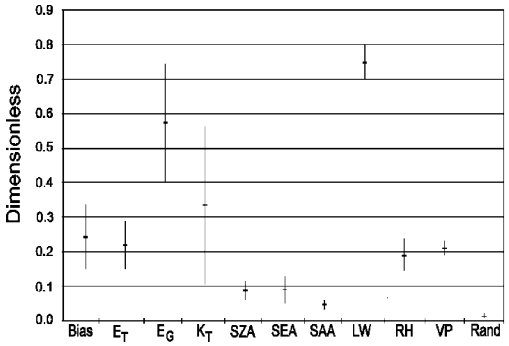

Fig. 2. Final saliency metrics.

ditional meteorological parameters, like air temperature and atmospheric pressure, are not important as the neural-network input.

The pattern selection technique was also used in one of the network constructions. There are two main reasons for its use: (i) when the available training database is really huge, the training process may be too slow and (ii) if some types of patterns are too frequent, but do not contain relevant information, they may "hide" the less frequent but very relevant patterns and consequently the final model may have a poor performance. Here, the hourly diffuse solar-radiation values are more or less equally distributed over the whole range and therefore a good network should perform equally well in the entire spectrum of output values, as a contrast to the pollution networks where a good model must predict well the peaks of concentration.

Table 1 summarizes the experiments performed and the most successful combination of input features, obtained after several trials. The output features were the hourly diffuse over global solar-radiation fraction.

Table 1
Experiment descriptions

	Experiment I	Experiment II	Experiment III
Input features			
E_T	Yes	Yes	Yes
E_D	Yes	Yes	Yes
K_T	Yes	Yes	Yes
LW	Yes	**No**	Yes
RH	Yes	Yes	Yes
SEA	Yes	Yes	Yes
SZA	Yes	Yes	Yes
SAA	Yes	Yes	Yes
VP	Yes	Yes	Yes
Selected patterns	No	No	**Yes**

5. Results

In all the experiments performed here, the standard back-propagation algorithm was used with a learning rate of 0.5 and momentum of 0.9. Previous works show that this selection of parameters leads to a quick and effective learning [26]. The networks were trained using almost 4 years of data (January 1998 → September 2001) and verified using 1-year of data (2002) that was not presented during the network training-period.

The first network (Experiment I) was trained with all available input features. To verify the importance of the long-wave radiation as an input feature, Experiment II was performed using as input all the input features used in Experiment I except for long-wave radiation.

To try to improve the network performance, the final experiment (Experiment III) was similar to Experiment I but included a pattern-selection technique. The idea was to develop the reconstruction of the patterns with high values of diffuse solar-radiation. Therefore, the neural network was trained with a higher percentage of patterns having diffuse solar-radiation greater than unity. For that reason, it was used only 40% randomly of the patterns with diffuse solar-radiation less than unity and all patterns with higher values of solar radiation.

5.1. Performance evaluation

To evaluate the performance of the MLP neural-networks, for the City of São Paulo, a statistical comparison is performed using the indicator proposed by Stone [16], a *t*-statistic (t_S). This indicator is used along with two other well-known parameters: MBE and RMSE. Both MBE and RMSE have been specially employed as adjustments of the solar-radiation models [3,11,28–30]. The RMSE and the MBE are defined as follows:

$$\mathrm{MBE} = \left(\sum_{i=1}^{N} d_i / N \right),$$

and

$$\mathrm{RMSE} = \left(\sqrt[2]{\sum_{i=1}^{N} (d_i)^2 / N} \right).$$

Here, N is the total number of observations and d_i is the deviation between the ith calculated value and the ith measured value.

The test of the MBE provides information on long-term performance of models studied and, in general, a small MBE is desirable. The test on RMSE provides information on the short-term performance of the models, as it allows a term-by-term comparison of the actual deviation between the calculated value and the measured value [28]. However, it is possible to have a large value for the RMSE and, simultaneously, a small value for the MBE, and vice versa.

Therefore, Stone [16] introduces the t-statistic as a new indicator of adjustment between the calculated and measured data, defined as:

$$t_S = \left(\sqrt[2]{(N-1)\mathrm{MBE}^2/\left(\mathrm{RMSE}^2 - \mathrm{MBE}^2\right)} \right).$$

To determine whether a model's estimates are statistically significant, one has simply to determine a critical t_c value obtainable from standard statistical tables, e.g., t_c $(\alpha/2)$ at the α level of significance, and $N-1$ degrees of freedom [30].

A summary of the statistical parameters is shown in Table 2 for the values of E_{DF} obtained in Experiments I, I, III and using the correlation model obtained from [3]. The critical values are relative to a level of confidence of 95%. The worst statistical result is given by the diffuse-radiation hourly values derived for São Paulo using the correlation model. The best result was obtained by Experiment III, but it still is not inside the acceptance region. Once that the hourly values of solar radiation are very sensitive to the cloud cover, the improvement obtained in Experiment I when compared with Experiment II (without long-wave radiation) seems to confirm that the long-wave radiation can be used as a surrogate for the cloud cover over the region.

5.2. Comparison between MLP and correlation model

Hereafter, due to the best statistic performance of Experiment III, the discussion will be focused only on this experiment.

The dispersion diagrams between the hourly values of diffuse solar-radiation observed and obtained using MLP network are displayed in Fig. 3. The coefficient correlation obtained using MLP (Fig. 3(a); $r = 0.94$) is larger than that using the correlation model (Fig. 3(b); $r = 0.91$), so indicating the better performance of the MLP network.

Histograms of the differences between the solar diffuse-radiation synthetic and observed are shown in Fig. 4. The standard deviation and the mean-error value are also presented in the figure. In the case of MLP and of the correlation model, the

Table 2
Model statistics

	Sample size (h)	MBE (MJ m^{-2})	RMSE (MJ m^{-2})	t_S	t_c
Correlation model obtained from [3]	15258	−0.0169	0.193	11.16	1.96
MLP neural-network – Experiment I	2928	0.0116	0.121	5.19	1.96
MLP neural-network – Experiment II	2928	0.0291	0.152	10.63	1.96
MLP neural-network – Experiment III	2928	0.0110	0.155	3.86	1.96

t_c is given at a level of confidence of 95%.

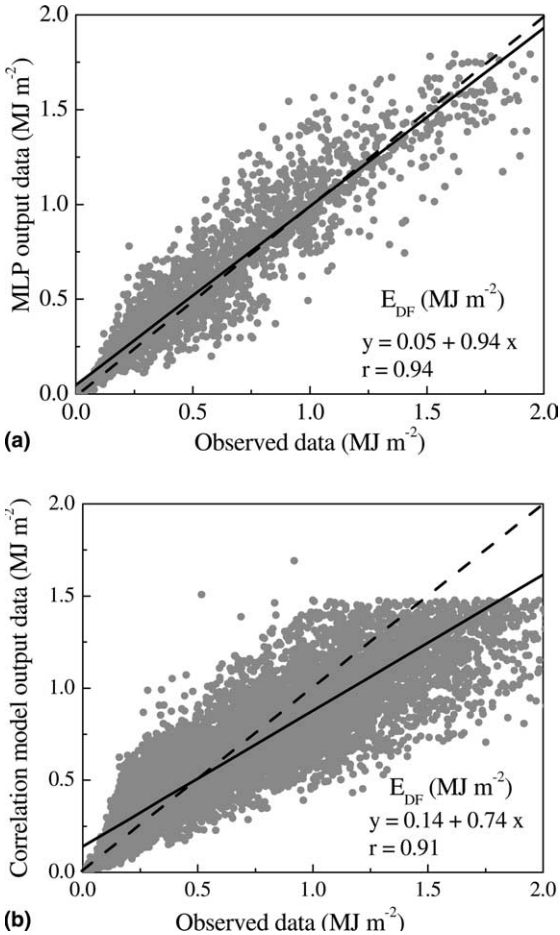

Fig. 3. Dispersion diagram between the hourly values of diffuse radiation observed and (a) using MLP based on 2928 pairs of points and (b) using the correlation model based on 15,258 pairs of points (from [3]). Dashed line corresponds to diagonal and continuous line corresponds to curve fitted by least squares method. The corresponding linear equations are indicated in the bottom of each diagram and r is the correlation coefficient.

standard deviations are, respectively, 0.132 and 0.182. In both cases, the mean values are in the vicinity of zero demonstrating a good performance of the MLP network.

The correlation between the diffuse fraction and clearness index can be displayed in terms of K_T–K_{DF} scatter diagrams. Fig. 5(a) shows K_T observed in São Paulo versus K_{DF} obtained using a MLP network, based on 2928 pairs of points. Fig. 5(b) displays K_T and K_{DF} observed values, based on 15,258 pairs of points, obtained from [3].

To characterize objectively the climatic behaviour of the diffuse solar-radiation at São Paulo, a fourth-degree polynomial was fitted through the data points in the K_T

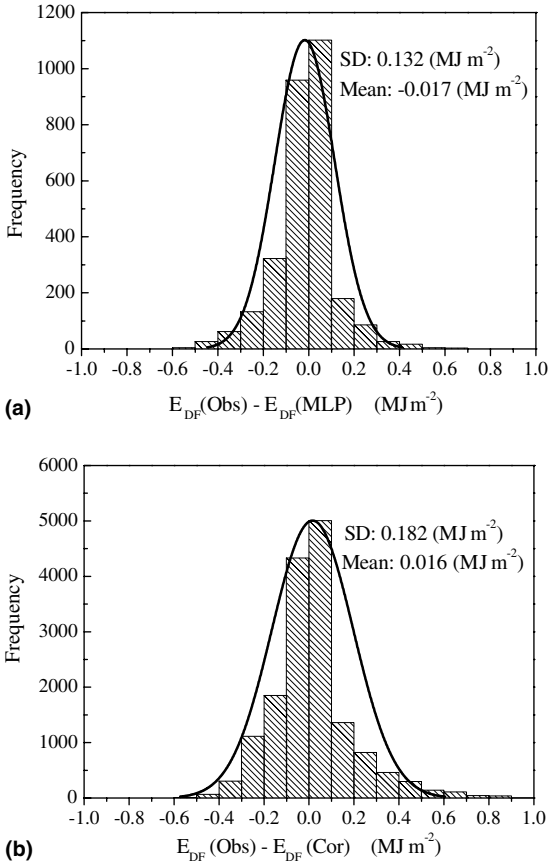

Fig. 4. Histogram of diffuse solar-radiation difference between observed and modeled values. (a) MPL based on 2928 points and (b) correlation model based on 15,258 points (from [3]). "SD" denotes the standard deviation and "mean" the average error.

versus K_{DF} diagrams (Fig. 5). This choice was based on the fact that most of the expressions, available in the literature for hourly values, are fourth-degree polynomials [3,7,9,31] allowing a straightforward comparison with previous works. The polynomial obtained using the data of Experiment III (Fig. 5(a), continuous line) is:

$$K_{DF} = 0.90 + 1.10(K_T) - 4.50(K_T)^2 + 0.01(K_T)^3 + 3.14(K_T)^4.$$

Oliveira et al. [3] obtained the polynomial expression (Fig. 5(b), dashed line):

$$K_{DF} = 0.97 + 0.80(K_T) - 3.00(K_T)^2 + 3.10(K_T)^3 + 5.20(K_T)^4.$$

The resemblance between the observed and synthetic polynomial curves (dashed and continuous lines in Fig. 5) indicates that the neural-network generated data preserve the regional climate feature of São Paulo.

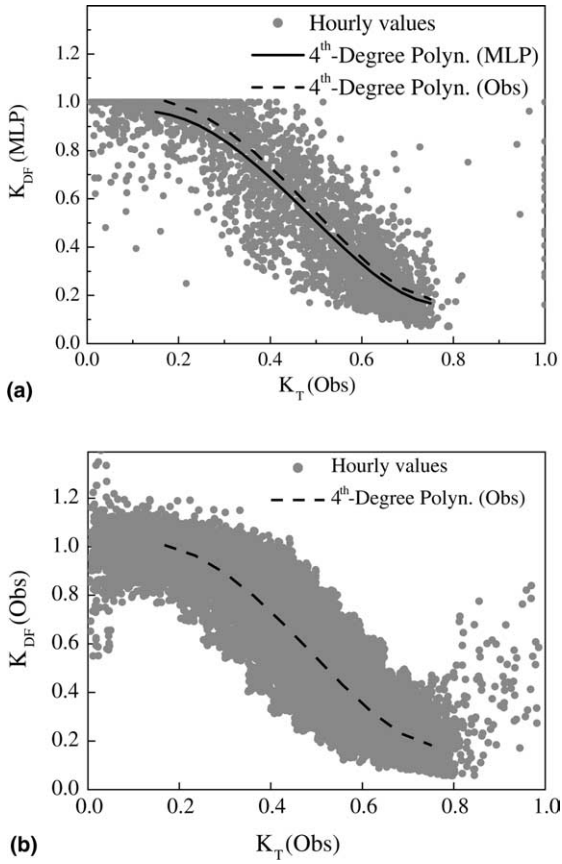

Fig. 5. K_T scatter diagram for hourly values of solar radiation. (a) K_{DF} obtained using MLP, based on 2928 pairs of points and (b) K_{DF} observed in São Paulo City, based on 15,258 pairs of points (from [3]). The continuous and dashed lines display the fourth-degree polynomial curves obtained, respectively, from MLP and [13].

6. Discussion and conclusion

In this paper, a methodology for generating a synthetic series of hourly values of the diffuse solar-radiation based on a neural network called multilayer perceptron is presented. A time series of almost 4 years of data was used to train MLP neural networks and 1 year of data was generated and used in the statistical analysis. The MLP methodology is based on the possibility of implicitly employing information associated with the problem without knowing the existing relationships between different variables and sources of information.

The best result was obtained by Experiment III (which includes the long-wave radiation and uses pattern selection technique) whereas it is still not inside the acceptance region of the *t*-statistic test. A polynomial expression was obtained fitting a

fourth-degree polynomial through the data points of K_T observed for São Paulo versus K_{DF} obtained using the MLP network. The resemblance between the observed and synthetic curves indicates that the neural-network generated data preserve the feature of the regional climate of São Paulo.

A significant result is the importance of atmospheric long-wave radiation as a surrogate for the cloud-cover information on the regional scale, a very difficult parameter to measure and express in diffuse solar-radiation models. By contrast, traditional meteorological parameters, like air temperature and atmospheric pressure, are not as important as long-wave radiation.

Acknowledgements

This research was sponsored by CNPq (Conselho Nacional de Desenvolvimento Científico e Tecnológico) during the collaboration program Brazil-Slovenia (Proc. CNPq No. 490017/02-9). On the Slovenian side, the research was sponsored by the AMES company and the Slovenian Ministry for school, science and sport during the same colaboration program.

References

[1] Collares-Pereira M, Rabl A. The average distribution of solar radiation – correlation between diffuse and hemispherical and between daily and hourly insolation values. Solar Energy 1979;22:155–64.
[2] González J-A, Calbó J. Influence of the global radiation variability on the hourly diffuse fraction correlations. Solar Energy 1999;65(2):119–31.
[3] Oliveira AP, Escobedo JF, Machado AJ, Soares J. Correlation models of diffuse solar-radiation applied to the City of São Paulo (Brazil). Appl Energy 2002;71(1):59–73.
[4] Iqbal M. An introduction to solar radiation. Academic Press; 1983. 390 pp.
[5] Liu BYH, Jordan RC. The interrelationship and characteristic distribution of direct, diffuse and total solar radiations. Solar Energy 1960;4:1–9.
[6] Collares-Pereira M, Rabl A. The average distribution of solar radiation – correlation between diffuse and hemispherical and between daily and hourly insolation values. Solar Energy 1979;22:155–64.
[7] Erbs DG, Klein SA, Duffie JA. Estimation of the diffuse-radiation fraction for hourly, daily and monthly-average global radiations. Solar Energy 1982;28:293–302.
[8] Satyamurti VV, Lahiri PK. Estimation of symmetric and asymmetric hourly global and diffuse radiations from daily values. Solar Energy 1992;48:7–14.
[9] Jacovides CP, Hadjioannou L, Passhiardis S, Stefanou L. On the diffuse fraction of daily and monthly global radiation for the Island of Cyprus. Solar Energy 1996;56:565–72.
[10] LeBaron B, Dirmhirn I. Strengths and limitations of the Liu and Jordan model to determine diffuse from global irradiance. Solar Energy 1983;31:167–72.
[11] Soler A. Dependence on latitude of the relation between the diffuse fraction of solar radiation and the ratio of global-to-extraterrestrial radiation for monthly average daily values. Solar Energy 1990;44:297–302.
[12] Rumelhart DE, Hilton GE, Williams RJ. Learning internal representation by error propagation. In: Rumelhart DE, McClelland JL, editors. Parallel distributed processing: explorations in the microstructure of cognition, vol. 1. Cambridge, MA: MIT Press; 1986.
[13] Lawrence J. Data preparation for a neural network. Artif Intell Expert 1991:34–41.
[14] Sfetsos A, Coonick AH. Univariate and multivariate forecasting of hourly solar-radiation with artificial-intelligence techniques. Solar Energy 2000;68(2):169–78.

[15] López G, Rubio MA, Martinez M, Batlles FJ. Estimation of hourly global photosynthetically-active radiation using artificial neural-network models. Agri Forest Meteorol 2001;107:279–91.
[16] Stone RJ. Improved statistical procedure for the evaluation of solar-radiation estimation models. Solar Energy 1993;51:289–91.
[17] Oliveira AP, Escobedo JF, Machado AJ, Soares J. Diurnal evolution of solar radiation at the surface in the City of São Paulo: seasonal variation and modeling. Theoret Appl Climatol 2002;71(3-4):231–49.
[18] Oliveira AP, Escobedo JF, Machado AJ. A new shadow-ring device for measuring diffuse solar radiation at the surface. J Atmos Oceanic Technol 2002;19(5):698–708.
[19] Dana G. Procedures for correcting Eppley pyrgeometer data; 1996. Available from http://huey.colorado. edu/LTER/datasets/meteorology/pyrgeometer.html.
[20] Fairall CW, Persson POG, Bradley EF, Payne RE, Anderson SP. A new look at calibration and use of Eppley precision infrared radiometers. Part I: Theory and application. J Atmos Oceanic Technol 1998;15:1229–42.
[21] Reda I, Hickey JR, Stoffel T, Myers D. Pyrgeometer calibration at the National Renewable Energy Laboratory (NREL). J Atmos Solar-Terrestrial Phys 2002;64:1623–9.
[22] Schalkoff R. Pattern recognition: statistical structural and neural approaches. New York: Wiley; 1992.
[23] Hornik K. Approximation capabilities of multilayer feedforward networks. Neural Networks 1991;4:251–7.
[24] Gardner MW, Dorling SR. Artificial neural-networks (the multilayer perceptron) – a review of applications in the atmospheric Sciences. Atmos Environ 1998;32:2627–36.
[25] Bonar M, Mlakar P. Improvement of air-pollution forecasting models using feature determination and pattern selection strategies. In: Gryning S-E, Chaumerliac N, editors. Air-pollution modeling and its application XII (NATO challenges of modern society). New York, London: Plenum Press; 1998. p. 725–26.
[26] Mlakar P, Bonar M. Perceptron neural-network-based model predicts air pollution. In: Adeli H, editor. Intelligent Information Systems IIS'97, Grand Bahama Island, Bahamas, December 8–10, 1997. Proceedings. Los Alamos, CA: IEEE Computer Society; 1997. p. 345.
[27] Mlakar P. Determination of features for air-pollution forecasting models. In: Adeli H, editor. Intelligent Information Systems IIS'97, Grand Bahama Island, Bahamas, December 8–10, 1997. Proceedings. Los Alamos, CA: IEEE Computer Society; 1997. p. 350–54.
[28] Halouani N, Ngguyen CT, Vo-Ngoc D. Calculation of monthly average global solar radiation on horizontal surfaces using daily hours of bright sunshine. Solar Energy 1993;50(3):247–58.
[29] Ma CCY, Iqbal M. Statistical comparison of solar radiation correlations. Monthly average global and diffuse radiation on horizontal surfaces. Solar Energy 1984;33(2):143–8.
[30] Targino ACL, Soares J. Modeling surface energy-fluxes for Iperó, SP, Brazil: an approach using numerical inversion. Atmos Res 2002;63(1):101–21.
[31] Newland FJ. A study of solar-radiation modes for the coastal region of South China. Solar Energy 1989;43:227–35.